Chemistry–A European Journal
Research Article
doi.org/10.1002/chem.202301642
Chemistry Europe
European Chemical Societies Publishing
www.chemeurj.org

Antimalarial Agents Derived from Metal-Amodiaquine Complexes with Activity in Multiple Stages of the *Plasmodium* Life Cycle

Legna Colina-Vegas,*[a] Mariana da Cruz B. Silva,[b] Caroline de Souza Pereira,[c] Ariane Isis Barros,[d] Joaquim Araújo Nobrega,[e] Maribel Navarro,[c] Matthias Rottmann,[f, g] Sarah D'Alessandro,[h] Nicoletta Basilico,[i] Alzir Azevedo Batista,[e] and Diogo R. M. Moreira*[b]

Malaria is the one of the deadliest infectious diseases worldwide. Chemically, quinolines are excellent ligands for metal coordination and are deployed as drugs for malaria treatment. There is a growing body of evidence indicating that metal complexes can be conjugated with antimalarial quinolines to be used as chemical tools to overcome the disadvantages of quinolines, improving their bioactive speciation, cellular distribution, and subsequently broadening the spectrum of activity to multiple stages of the complex *Plasmodium* life cycle. In this study, four novel complexes of ruthenium(II)- and gold(I)-containing amodiaquine (AQ) were synthesized, and a careful chemical characterization revealed the precise coordination site of AQ to the metals. Their speciation in solution was investigated, demonstrating the stability of the quinoline-metal bond. Ru^{II}- and Au^{I}-AQ complexes were demonstrated to be potent and efficacious in inhibiting parasite growth in multiple stages of the *Plasmodium* life cycle as assayed in vitro and in vivo. These properties could be attributed to the ability of the metal-AQ complexes to reproduce the suppression of heme detoxification induced by AQ, while also inhibiting other processes in the parasite life cycle; this can be attributed to the action of the metallic species. Altogether, these findings indicate that metal coordination with antimalarial quinolines is a potential chemical tool for drug design and discovery in malaria and other infectious diseases susceptible to quinoline treatment.

Introduction

Malaria is one of the oldest diseases affecting humans and holds a unique place in human history. New immunological and molecular experiments performed on ancient skeletal samples have confirmed the presence of malaria for at least the last 4800 years.[1,2] In the 20th century, this parasitic disease is thought to have caused between 2 and 5% of all human fatalities. According to the latest malaria report, published in 2022, the disease was estimated to be the cause of 619000 deaths in 2021, 77% of whom were children under five years of age, out of a total of 247 million cases.[3]

Malaria is transmitted through the bites of female *Anopheles* mosquitoes containing one of the five species of parasites that infect humans (*Plasmodium falciparum, Plasmodium vivax, Plasmodium ovale, Plasmodium malaria and Plasmodium knowlesi*). As an infected mosquito bites a human, it injects *Plasmodium* parasites into the bloodstream in the form of sporozoites (Figure 1), which travel to liver cells, where they multiply asexually and mature into schizonts, which rupture

[a] *Prof. L. Colina-Vegas*
Instituto de Química
Universidade Federal do Rio Grande do Sul
Porto Alegre, CP 91501–970, RS (Brazil)
E-mail: legna.vegas@ufrgs.br

[b] *M. da Cruz B. Silva, Dr. D. R. M. Moreira*
Instituto Gonçalo Moniz, FIOCRUZ
Salvador, CEP 40296–710, BA (Brazil)
E-mail: diogo.magalhaes@fiocruz.br

[c] *Dr. C. de Souza Pereira, Prof. M. Navarro*
Departamento de Química
Universidade Federal de Juiz de Fora
Juiz de Fora, CP 36036–900, MG (Brazil)

[d] *Dr. A. Isis Barros*
Departamento de Solos e Engenharia Rural
Universidade Federal de Mato Grosso
Cuiabá, CEP 78060–900, MT (Brazil)

[e] *Prof. J. Araújo Nobrega, Prof. A. Azevedo Batista*
Departamento de Química
Universidade Federal de São Carlos
São Carlos, CP 13565–90, SP (Brazil)

[f] *Dr. M. Rottmann*
Swiss Tropical & Public Health Institute
4123 Allschwil (Switzerland)

[g] *Dr. M. Rottmann*
University of Basel
4001 Basel (Switzerland)

[h] *Dr. S. D'Alessandro*
Dipartimento di Scienze Farmacologiche e Biomolecolari
Università degli Studi di Milano
Milan, 20133 (Italy)

[i] *Prof. N. Basilico*
Dipartimento di Scienze Biomediche, Chirurgiche e Odontoiatriche
Universitá degli Studi di Milano
Milan, 20133 (Italy)

Supporting information for this article is available on the WWW under https://doi.org/10.1002/chem.202301642

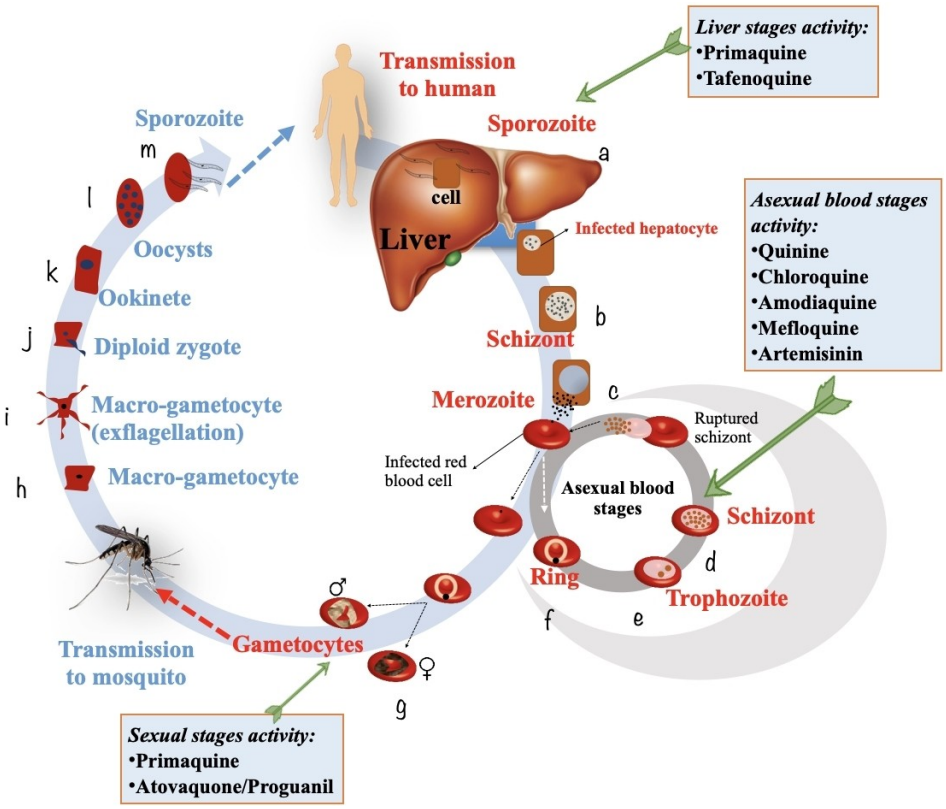

Figure 1. *Plasmodium* life cycle and the stages where antimalarial drugs act.

and release merozoites. Following this initial liver replication stage (exo-erythrocytic schizogony), the merozoites infect red blood cells, starting asexual replication in erythrocytes. This stage is responsible for the disease's clinical symptoms and is known as erythrocytic schizogony. Some of the infected blood cells stop reproducing asexually and transform into gametocytes, which are the sexual forms of the parasite that circulate in the bloodstream, rather than replicating. When a mosquito bites an infected person, it consumes gametocytes, which later mature into sporozoites and restart the life cycle.[4]

The main symptoms of uncomplicated malaria are fever, sweating, chills, headache, fatigue, diarrhea, nausea, and breathing problems. It can progress to cause severe anemia or the most complicated form of malaria (cerebral malaria). Multifaceted approaches have been used to control malaria transmission, including insecticide-treated bed nets and indoor residual spraying. The use of such approaches is believed to have averted around 800 millions of cases between 2004 and 2019.[5] In 2021, an important development in malaria prevention was the WHO's recommendation of the malaria vaccine RTS,S/AS01 (tradename Mosquirix), the world's first malaria vaccine administered to children living in sub-Saharan Africa and other regions, in four doses: the first at five months of life, the second at eight months, the third at 11 months, and the fourth at 18 months.[6]

Treatment with adequate and timely chemotherapy prevents severe disease, thus reducing the number of deaths and eliminating sources of infection for the vector. The set of antimalarial drugs includes molecules that differ widely in the way they are used, mainly due to differences in regional patterns of pathogen resistance. Except for complicated malaria, these drugs are administered orally as combinations, the components of which are chosen based on local resistance and other factors such as strains and species of parasite.[7]

The quinoline class of antimalarials includes the drugs that are most commonly used in the treatment of infected persons. They act on the erythrocytic stages of the parasites, especially on trophozoites, which can catabolize hemoglobin and release the heme [Fe^{II}PPIX]. Released heme is rapidly oxidized to hematin [H_2O-Fe^{III}PPIX], which is toxic to the parasite in its free (i.e., soluble) state. The parasite's main detoxification mechanism is through the crystallization of hematin, generating crystals of hemozoin, which are not toxic to the parasite. Blocking the polymerization of hematin has been the main molecular target for antimalarial drugs, including the quinoline chemical class.[8] Recently, their mode of action was investigated in vivo by mapping *P. falciparum*-infected red blood cells treated with a bromo analog of chloroquine using non-destructive X-ray microscopy, revealing that the analog covered a significant proportion of the sites at the surface of hemozoin crystals in the digestive vacuole of the *Plasmodium* parasites, thereby confirming that blocking hematin polymerization in the erythrocytic stage is the main mechanism of action of antimalarial quinolines.[9]

The discovery of strains of *P. falciparum* that are resistant to chloroquine (CQ) has driven researchers to search for alternative

drugs. Transition metals have a remarkable ability to form multiple coordination bonds with lone pairs of electrons from nitrogen, oxygen, and sulfur present in antimalarial drugs, especially quinolines. Examples of these have been demonstrated since the mid-1990s by at least four independent research groups around the world.[10–20] Biot reported the incorporation of ferrocenyl moieties into the structures of antimalarial drugs to make organometallic compounds containing quinolines,[10–12] the most notable example being the antimalarial drug ferroquine (FQ). In the same decade, the groups of Sanchez-Delgado and of Navarro reported on Ru-CQ and Rh-CQ complexes that showed in vitro activity against *P. falciparum*.[13–17] Smith and Nordlander have also reported metal–quinoline complexes but using synthetically modified quinolines.[18,19] In general, all these metal-CQ complexes possess the ability to disrupt the heme detoxification pathway of the malaria parasite as a mode of action. The gold(I) complex $[Au(CQ)(PPh_3)]PF_6$ displayed greater in vitro and in vivo activity than the reference drug CQ, with no evidence of cell toxicity.[14,15] Subsequently, our research group reported that Ru-CQ and Pt-CQ complexes have a wide range of inhibitory activity against multiple stages of the *Plasmodium* life cycle, including sporozoites and gametocytes.[20,21]

As part of our ongoing efforts to improve and understand the antimalarial activity of metal-quinoline complexes, we decided to explore the substitution of CQ by amodiaquine (AQ) as a ligand in ruthenium and gold complexes. AQ is an effective drug in regions with low prevalence of drug-resistant parasites, including the Latin America.[22,23] For accessing parasite susceptibility, AQ as well as its main metabolite, monodesethylamodiaquine (dAQ), are typically employed for in vitro assays, while AQ is typically employed for in vivo assays of pharmacodynamics/pharmacokinetics.[22,23] In Figure 2, we highlight some of the medicinal organic and inorganic chemistry approaches for modifying the AQ structure. Some of these modifications have yielded organically synthetic analogues of AQ, such as fluoro-AQ,[23] pyrrolidine-AQ,[24] and benzoxazole-AQ.[25] In this work, we present the synthesis, characterization, in vitro and in vivo antiplasmodial activity and heme detoxification suppression of three novel ruthenium- and one gold-AQ complexes.

Results

Synthesis and characterization

Three ruthenium(II)-AQ complexes (**1-3**) and one gold(I)-AQ complex (**4**) were synthesized by the Schlenk technique in an argon atmosphere by the substitution of a chloride ligand from the metal precursor for one AQ molecule. AQ free base is a greenish solid that is extracted from the reaction between amodiaquine dihydrochloride dehydrate and $NaHCO_3$. This step is performed in order to release its nitrogen atoms for metal coordination. To stabilize the cationic species, PF_6^- was

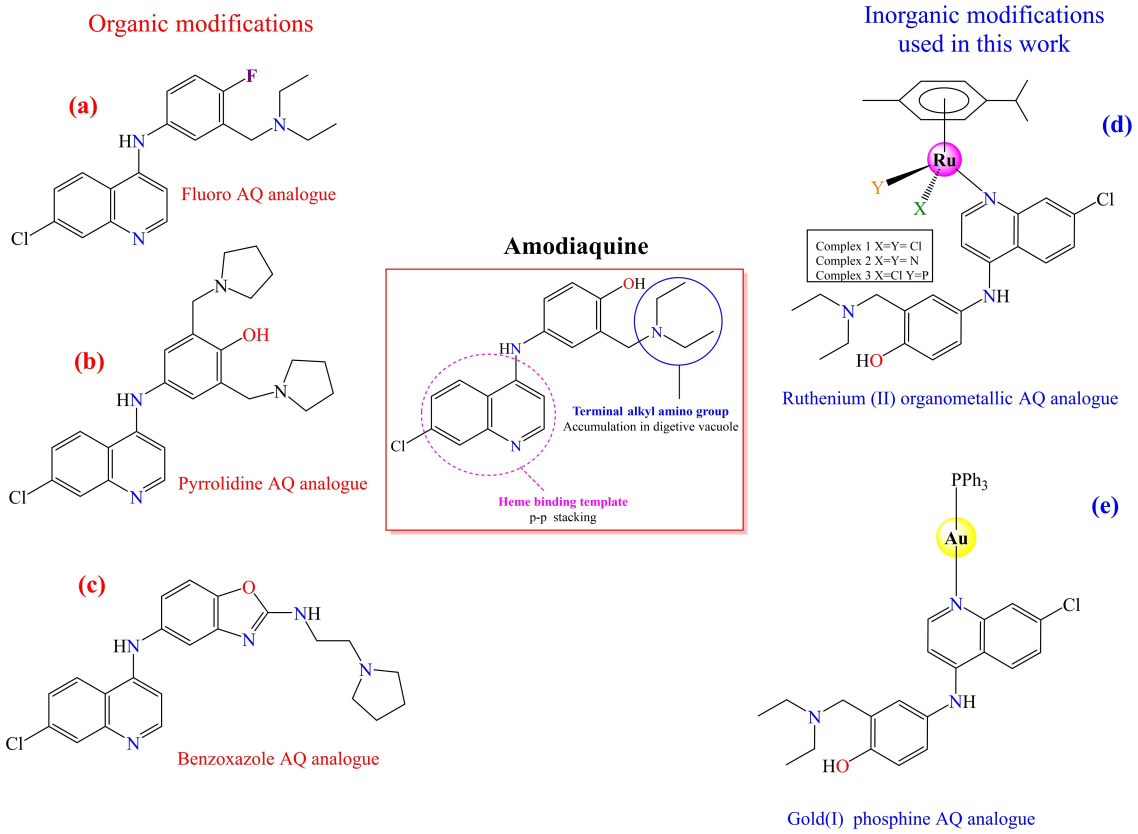

Figure 2. Center: map of the structure–activity relationships of AQ for antimalarial activity. Left: Medicinal chemistry using organic synthesis approaches to modify AQ. Right: Medicinal chemistry using inorganic metal–ligand coordination approaches to form new metal-AQ complexes.

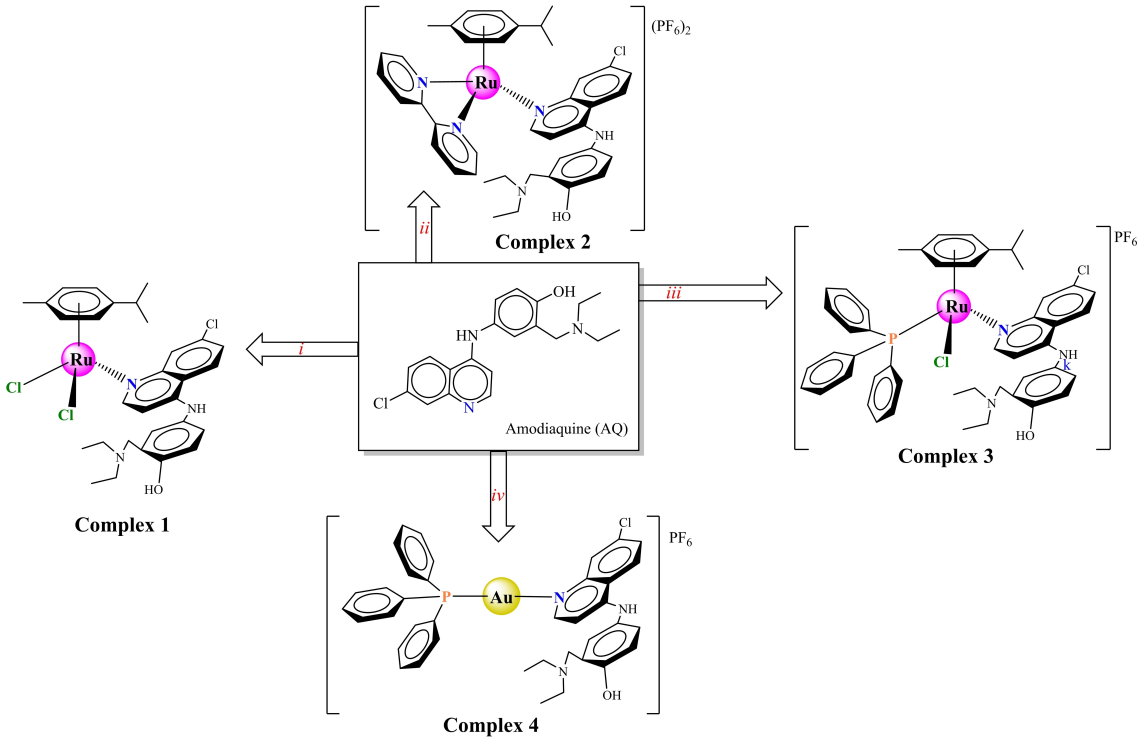

Figure 3. Synthetic procedures for the Ru^{II} and Au^{I} complexes containing AQ. *i*: $(CH_3)_2CO$, 60 °C, 2 h, (75% yield); *ii*: MeOH, NH_4PF_6, 70 °C, 24 h, (68% yield); *iii*: MeOH, CH_2Cl_2, NH_4PF_6, 70 °C, 6 h, (82% yield); *iv*: CH_3CN, $AgPF_6$, 70 °C, 12 h, (67% yield).

employed as a counter-ion. A schematic route of the synthesis is shown in Figure 3.

In the solid state, the complexes $[Ru(Cl)_2(AQ)(\eta^6\text{-}p\text{-cymene})]$ (**1**), $[Ru(AQ)(\eta^6\text{-}p\text{-cymene})(2,2'\text{-bipyridine})](PF_6)_2$ (**2**), $[Ru(Cl)(AQ)(\eta^6\text{-}p\text{-cymene})(PPh_3)]PF_6$ (**3**), and $[Au(AQ)(PPh_3)]PF_6$ (**4**) were yellowish or brownish in color. These solids were stable when exposed to light and air, and they were insoluble in water, hexane, and diethyl ether, but soluble in methanol, acetone (except for complex **1**), DMSO, dichloromethane, acetonitrile, and chloroform. Elemental analyses confirmed the proposed molecular formulas (Table S1 in the Supporting Information).

The molar conductivity value of $10.50 \pm 1.50\ \Omega^{-1}\,cm^2\,mol^{-1}$ for complex **1** is too low for a 1:1 electrolyte in ethanol (35-45 $\Omega^{-1}\,cm^2\,mol^{-1}$), suggesting that it is a neutral compound; but it increases rapidly due to one chloride ion present outside the coordination sphere after solvent coordination (Figure 4). This exchange was observed for coordinating polar solvents, such as CH_3CN and DMSO. The phenomenon of solvent coordination in organometallic complexes has been reported for similar compounds, such as [Ru(arene)(monodentate-ligand)$(Cl)_2$] and [Ru(arene)(bidentate-ligand)(Cl)]X.[26,27] For complex (**2**), the conductivity value of $173.10 \pm 2.70\ \Omega^{-1}\,cm^2\,mol^{-1}$ was in the range for a 2:1 electrolyte in acetone (160-200 $\Omega^{-1}\,cm^2\,mol^{-1}$), while complexes **3** and **4** the conductivity values of 121.50 ± 4.3 and $124.30 \pm 1.70\ \Omega^{-1}\,cm^2\,mol^{-1}$, respectively, were in the range for a 1:1 electrolyte in acetone (100–140 $\Omega^{-1}\,cm^2\,mol^{-1}$).[28] Importantly, the molar conductivity values did not vary over a period of 24 h for these three complexes, suggesting no ligand exchange reaction took place.

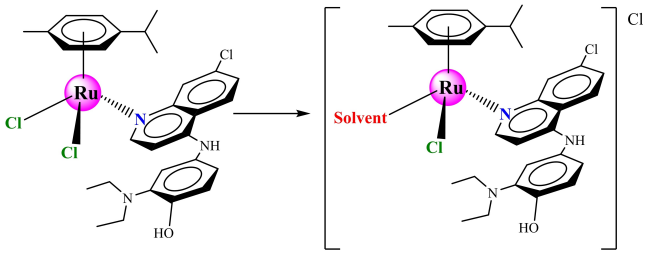

Figure 4. Coordination reaction of a polar solvent with the complex $[Ru(Cl)_2(AQ)(\eta^6\text{-}p\text{-cymene})]$ (**1**), resulting in the dissociation of the chloride and the coordination of the solvent in the metallic sphere.

The absorption spectrum in the UV-vis region of each complex showed an intense high-energy band around 250 nm, which was assigned to n→π* and π→π* transitions of the quinoline ligand. A broad band in the 340–400 nm region was assigned to metal-to-ligand charge transfer transition from the metal to the ligand (π*).[29] The absorption bands in the infrared region for the metal complexes showed the characteristic signals of amodiaquine (AQ), triphenylphosphine (PPh_3), 2,2′-bipyridine (bipy), and *p*-cymene (*p*Cy) ligands in the range of 3430–3414 cm^{-1} (O–H), 3350–3240 cm^{-1} (N–H), 2855–2850 cm^{-1} (C–H aliphatic), 1618–1608 cm^{-1} (C=C), 1576–1567 cm^{-1} (C=N), and 750–745 cm^{-1} (C–Cl). The presence of the PPh_3 ligand was confirmed by symmetric and asymmetric stretching of νP–C around 1090 and 1000 cm^{-1}, respectively. Complexes **2**–**4** also exhibited characteristic bands, which we

attempted to attribute to ν(P–F) and δ(P–F) for the counter-ion PF_6^- in the 855–842 cm^{-1} and 556–528 cm^{-1} ranges, respectively.[30]

The ESI-MS(+) spectra for the cationic complexes **1**, **2** and **3** presented a signal with an isotopic distribution typical of ruthenium at 567.9702, 427.0512 and 533.0748 *m/z*, respectively, which were attributed to $[RuC_{27}H_{30}Cl_2N_3O]^+$ for complex **1**, $[RuC_{18}H_{16}ClN_3O]^+$ for complex **2** and $[RuC_{28}H_{29}ClP]^+$ for complex **3**, respectively. Similarly, the ESI-MS(+) spectra for the cationic complex **4** revealed a signal with an isotopic distribution typical of gold at 841.2067 *m/z*, which was attributed to $[AuC_{34}H_{27}N_3OP]^+$ (Figures S2–S5).

Subsequently, the complexes were characterized by: 1D multinuclear NMR; ^1H, $^{13}C\{^1H\}$, $^{31}P\{^1H\}$), and 2D correlation spectroscopy (COSY $^1H,^1H$); heteronuclear single quantum correlation (HSQC $^{13}C,^1H$); and heteronuclear multiple-bond correlation (HMBC $^{13}C,^1H$). The ^1H NMR signals for the compounds were consistent with characteristic resonances, chemical shifts, signal multiplicities, and coupling constants of AQ and auxiliary ligands (*p*Cy, PPh_3, and bipy). A relative integral ratio of 1:1 was often observed (Figures S2–S5).

In the ^1H NMR spectra of complexes **1–4**, the hydrogens of the aliphatic group of AQ and *p*-cymene (*p*Cy) were observable at low frequencies (δ 1–4 ppm). Doublets were observed at low frequencies (δ 5–6 ppm) and assigned to the aromatic hydrogens of the *p*Cy, as well as at high frequencies (δ 7–10 ppm), assigned to the hydrogens of PPh_3, AQ, and bipy. A chemical shift of the *p*Cy signals to a lower magnetic field is caused due to a remotion of electronic density of the bipy in the metallic center. The NH and OH signals remained unaltered in the AQ coordinated to the metal, suggesting that AQ binds to the metal center through the aminoquinoline N1 atom. N1 is a good donor site for coordination and this kind of coordination has been reported in other metal-quinoline complexes.[18,27]

Figure 5a–d shows a selected region in the ^1H NMR spectrum containing the signals of the aromatic hydrogens H_5, H_6, H_8, and H_9 in the *p*-cymene (*p*Cy) ring for the precursor and their metal-AQ complexes. The spectra of both the precursor $[Ru(Cl)_2(p\text{-}Cy)]_2$ and complex **1** show two pairs of doublets at δ 5.7–5.8 ppm attributed to *p*Cy. These characteristic doublets are not affected after AQ is introduced (Figure 5a and b). In contrast, these two pairs of doublets at δ 5.9–6.2 ppm in the spectrum of complex **2** (Figure 5c) shift further downfield than the doublets in complex **1**. Similar behavior in signal shifting has been reported for $[Ru(Cl)(\eta^6\text{-}p\text{Cy})(bipy)]PF_6$ and $[Ru(CQ)(\eta^6\text{-}p\text{Cy})(bipy)](PF_6)_2$.[27] In the spectrum of complex **3** (Figure 5d), these signals were displayed as four pairs of doublets in the δ 5.0–6.0 ppm region, with a shift further into the upfield region than the doublets in complexes **1** and **2**. We attributed this pattern of signals to the stereogenic ruthenium center (Figure S6). The stereogenic ruthenium center has been reported for organometallic complexes such as $[Ru(Cl)(\eta^6\text{-}p\text{-cymene})(PPh_3)(L)]PF_6$ with L: clotrimazole and ketoconazole.[31] In all these examples, the complexes displayed the system [Mabcd], where M=Ru center and a, b, c, d are four different atoms bound to the metal, suggesting that this combination of bonds can promote non-equivalence in the ring of the *p*Cy group, therefore causing signal separation from two pairs of doublets into four pairs of doublets.[32]

The $^{31}P\{^1H\}$ NMR spectra of complexes **2**, **3**, and **4** display a heptet signal at δ −144.5 ppm attributed to the PF_6^- anion. For complexes **3** and **4**, a singlet was observed for the phosphorus from the PPh_3 group at δ 34 ppm and 32 ppm, respectively. The signals corresponding to the PPh_3 group in complexes **3** and **4** shifted when compared with the precursors $[Ru(Cl)_2(\eta^6\text{-}p\text{-cymene})(PPh_3)]$ and $[AuCl(PPh_3)]$ (Figure S7). We attribute this to AQ coordination. More specifically, the reason for this deshielding effect of the phosphine group in the $^{31}P\{^1H\}$ NMR is most likely due to the exchange of chlorido ligand (π- and σ-donors)

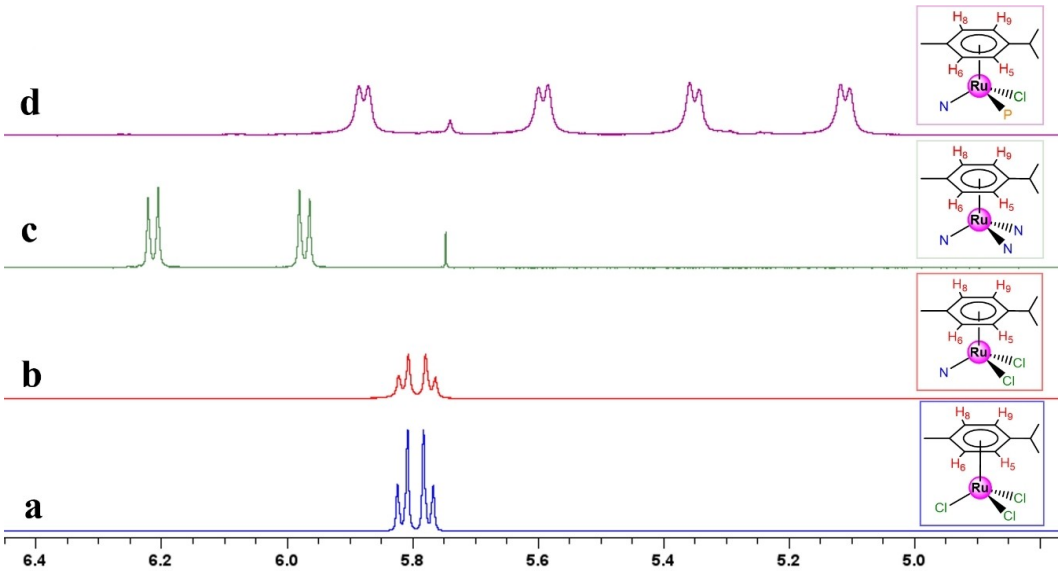

Figure 5. ^1H NMR spectra in $[D_6]$DMSO for a) the precursor $[RuCl_2(p\text{-cymene})]_2$ and metal–quinoline complexes b) **1**, c) **2**, and d) **3**, highlighting the aromatic signal of the *p*-cymene ligand (δ 5 to δ 6.4 ppm).

for 4-aminoquinoline (π-acceptor); this is broadly consistent with the literature.[27,33]

After chemical characterization, the chemical stability of the complexes in solution was determined. Except for complex **1**, all the complexes remained stable after incubation for 48 h at 37 °C in pure DMSO or in a mixture of DMSO and cell culture medium; no ligand exchange reactions were inferred by NMR and UV-vis analyses (Figures S8–S10). Importantly, no evidence was found to indicate that AQ underwent any kind of ligand exchange reaction or that the metal coordination to AQ, which is through its quinolinic nitrogen, changed upon addition of DMSO and cell culture medium.

In vitro potency and in vivo efficacy in inhibiting multiple stages of the Plasmodium life cycle

The antiplasmodial activity of the metal complexes **1**–**4** was first evaluated in vitro against three different strains of *P. falciparum* at the asexual blood stages, followed by an evaluation of in vitro activity against the sexual blood stages of *P. falciparum*, for which it was assayed against stage V gametocytes. Drug cytotoxicity toward mammalian cells was determined in murine macrophages (J774 cell line) and the hepatocellular carcinoma (HepG2 cell line). Subsequently, an in vivo evaluation of efficacy for the two more potent metal complexes was performed in *Plasmodium berghei*-infected mice in order to assess the blood schizonticide potential of the drugs. In all experiments, the potency and efficacy of metal complexes were compared to AQ treatment.

As can be seen in Table 1, both CQ-sensitive (NF54) and CQ-resistant (W2 and K1) strains of the asexual blood stages were quite susceptible to AQ treatment. Despite this susceptibility, it was important to assess the susceptibility of both CQ-sensitive and CQ-resistant strains to the metal complexes, since these could present cell permeation or distribution dissimilar to AQ, resulting in dissimilar antiplasmodial activity across different parasite strains. The screening of compounds revealed that across the three different parasite strains, there was no difference in susceptibility to the metal complexes, indicating that, like AQ, the metal complexes are able to inhibit the growth of all parasite strains. By comparing these results to ones reported in the literature,[20,21] we can infer that the nature of 4-aminoquinoline considerably increases the antimalarial activity of the metal complexes.

Table 1. In vitro antiparasitic activity of AQ and its metal complexes against asexual and sexual blood stages of *P. falciparum*.

Compounds	IC_{50} (mean, nM) for *P. falciparum*			
	Asexual blood stage[a]			Gametocytes V of 3D7 strain [b]
	NF54 (CQ-sensitive)	W2 (CQ-resistant)	K1 (CQ-resistant)	
1	6.3	3.2	12.6	> 10000
2	n.d.	12.0	n.d.	n.d.
3	21.7	8.3	7.7	8970
4	6.9	3.5	13.5	7380
amodiaquine	11.4	7.4	16.5	23600
chloroquine	7.5	430	114	> 20000

[a] Inhibitory concentration for 50% (IC_{50}) determined 72 h after incubation of asexual blood stages (asynchronous culture) with compounds using the tritiated hypoxanthine readout. [b] Inhibitory concentration for 50% (IC_{50}) determined 72 h after incubation of sexual blood stages (gametocytes, stage V) with compounds using the luciferase readout. Values were calculated as mean of two independent experiments. Amodiaquine free base; chloroquine diphosphate. n.d. = not determined; S.D. = standard deviation. All sigmoid curves are available in Figure S11.

After ascertaining this, we compared the potency of the antiplasmodial activity of AQ and the metal complexes **1**–**4**. We observed that complexes **2** and **3** were as potent as AQ, while complexes **1** and **4** were approximately twice as potent as AQ. While the asexual blood stages are quite susceptible to heme detoxification suppressors like AQ and CQ, the sexual blood stages (gametocytes) are much less susceptible to this class of drugs. However, bearing in mind that gametocytes are quite susceptible to methylene blue, a potent gametocidal redox-active drug,[34] we speculated that because of potential redox-based activity provided by transition metals,[35] the metal complexes **1**–**4** could display gametocidal activity. As we can see in Table 1, neither AQ nor the metal complexes **1**–**4** displayed gametocidal activity in low nanomolar concentrations, as observed for the asexual blood stages.

Further screening of cytotoxicity for mammalian cells and determination of the selectivity indexes (Table 2) revealed that metal complexes **3** and **4** were the most selective antiplasmodial agents, making an investigation of their efficacy in vivo worthwhile. Their efficacy as a blood schizonticidal agent was assessed in *P. berghei*-infected mice using a standard 4-day regime. The lowest dose capable of ensuring 50% survival in mice was set at 30 μmol AQ treatment per kg of animal weight (20.5 mg/kg), given intraperitoneally, while 15 μmol/kg is known to suppress parasitemia, but does not provide a cure. Based on this, this drug dosage range was chosen to evaluate metal complexes **3** and **4**.

As shown in Table 3, at 15 μmol/kg, compound **3** and AQ were efficacious in reducing parasitemia in mice, but they did not provide a cure. In this same dosage, compound **4** was efficacious in reducing parasitemia and in increasing animal survival in comparison to the untreated infected group. When complex **4** was increased to 30 μmol/kg, it was able to cure 70% of mice from a pool of two independent experiments, compared to the 50% cured after AQ treatment. Based on this, the efficacy displayed by complex **4** was twice as high as that of AQ treatment and the efficacy of complex **3** was half that of AQ treatment.

After ascertaining the efficacy of complex **3**, we decided to estimate the plasma and blood concentration of ruthenium in the uninfected mice treated with a bolus dose equivalent to the dose given to the *P. berghei*-infected mice. Evaluating the exposure to ruthenium in biological matrices is necessary in order to comprehend the pharmacokinetics of antimalarial ruthenium-based drugs. The use of mass spectrometry techniques such as inductively coupled plasma-mass spectrometry

Table 2. In vitro cytotoxicity of AQ and its metal-AQ complexes for mammalian cells and their selectivity profile.

Compounds	CC_{50} (mean ± S.D. [nM])[a]		Hemolysis in uRBC [%][b]	Selectivity index[c]	
	J774	HepG2		NF54	W2
1	3700 ± 100	> 50000	0	587	1156
2	9900 ± 400	> 50000	0	n.d.	825
3	6700 ± 700	25600 ± 4600	0	1763	807
4	4800 ± 800	8700 ± 1200	13.5 (11.2-16.7)	695	1371
amodiaquine	7400 ± 500	40500 ± 900	0	649	1000
chloroquine	37600 ± 3600	> 50000	0	5013	87

[a] Cytotoxic concentration for 50% (CC_{50}) against the murine macrophages of the J774 cell lineage and the human hepatocellular carcinoma of the HepG2 cell lineage, determined 72 h after incubation with compounds using the AlamarBlue readout. Values were calculated as mean ± S.D. of at least three independent experiments. [b] Percentage of hemolysis (in comparison to untreated samples) using uninfected human red blood cells (RBC). Compounds were tested at concentration of 5000 nM. Values are the mean (95% CI) of one single experiment. [c] Determined as CC_{50}/IC_{50} using CC_{50} values from J774 cells. Amodiaquine free base; chloroquine diphosphate. S.D., standard deviation.

Table 3. Efficacy of AQ and its metal-AQ complexes to suppress the parasitemia in *P. berghei*-infected mice.

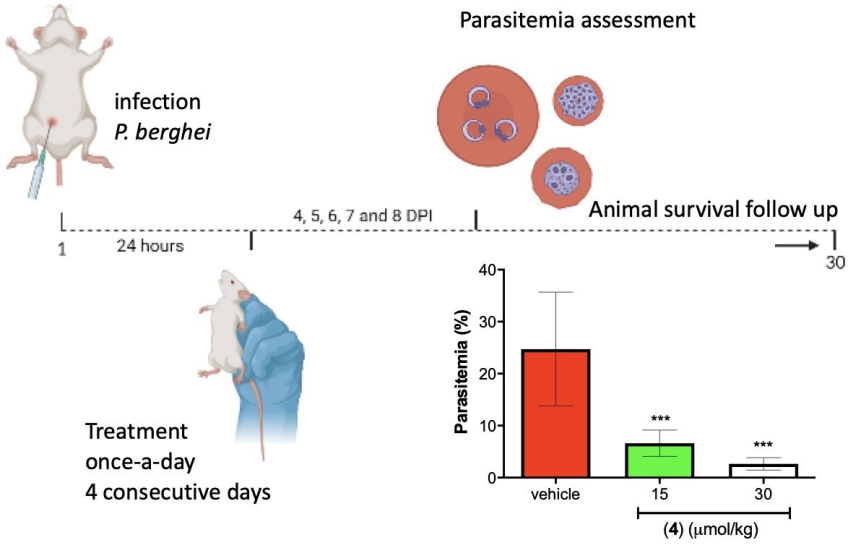

Groups	Dose μmol/kg [mg/kg] / I.P.	Parasitemia inhibition [%][a]	Median of animal survival [d]	Number of cured mice on 30 DPI [%]
vehicle	-,–	-,–	13	0
3	15 (15)	52.9 ± 2.38	16	0
3	60 (60)	95.3 ± 0.27	29[#]	60
4	15 (14.5)	70.6 ± 6.18	> 30[#]	50
4[b]	30 (29)	84.1 ± 2.73	> 30[#]	70
amodiaquine	15 (10.2)	55.3 ± 0.11	18	0
amodiaquine [b]	30 (20.5)	87.1 ± 1.59	28[#]	50

[a] Values are mean and standard deviation determined in comparison to vehicle group using $n = 5$/group and from one single experiment. [#] $p < 0.05$ (Log-rank and Mantel-Cox test) versus vehicle. [b] Values are from a pool of two independent experiments. D = days. DPI = days post-infection. I.P. = intraperitoneal injection. Amodiaquine dihydrochloride dihydrate. All raw data are available in Figure S12.

(ICP-MS) for detection and imaging of metallodrugs is an area of research that is being increasingly explored in the field of oncology,[36] but is less investigated in parasitic infectious diseases.

Complex **3** was chosen because of its strong efficacy plus the fact that the literature on ruthenium quantification of antimalarial metallodrugs in blood or plasma samples is relatively scarce. A time frame of 3 and 24 h was selected, given that typically the antimalarial drug AQ peaks in the plasma at 3 h and remains for at least 24 h before elimination. As can be seen in Figure 6, the ruthenium content was higher at 3 h than at 24 h post-treatment. Moreover, the ruthenium content was higher in the plasma than in the peripherical blood. Although we were not able to quantify the AQ content in the samples,

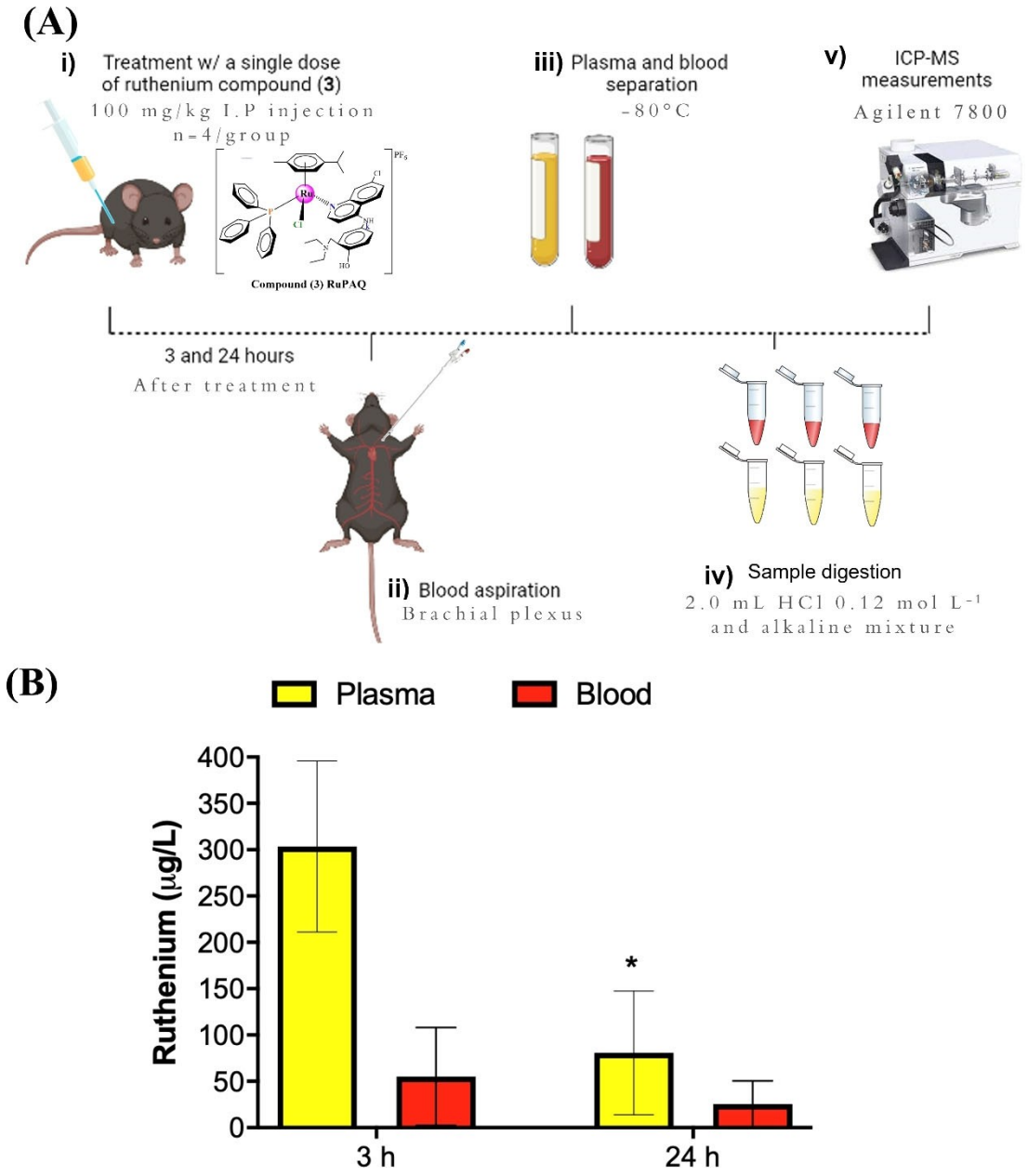

Figure 6. A) Experimental design. B) Results of the quantification of ruthenium by ICP-MS in plasma and blood. Uninfected C57BL/6 mice ($n=4$/group) were treated with a single dose of ruthenium compound RuPAQ (**3**; 100 mg/kg; 102 µmol/kg) by I.P. injection. At 3 and 24 h after treatment, samples were harvested and processed for determination of ruthenium content by ICP-MS. Values are the means and standard deviation. *$p<0.05$ (two-way ANOVA and Bonferroni post-test) versus 3 h data-point.

the observed kinetic profile and distribution of the ruthenium content in these samples is suggestive that the pharmacokinetic profile of complex **3** is similar to that of AQ.[22,24]

Mechanism of antiplasmodial activity

To study the potential of metal complexes **1**–**4** to suppress *Plasmodium* heme detoxification, their association constant (log *K*) with the soluble hemin chloride [Cl-Fe^{III}PPIX][37] and their ability to suppress formation of the β-hematin crystals were determined.[38] The main heme-detoxifying process in *Plasmodium* involves the crystallization of hematin into hemozoin, which prevents the accumulation of free and toxic heme in the parasite's digestive vacuole. The development of β-hematin crystals, the synthetic analogue of hemozoin, is known to be disrupted by antimalarial agents of historical significance and current therapeutic use, such as chloroquine, amodiaquine, and others.[8,9] It is proposed that this crystal formation is due to a π–π stacking interaction between the antimalarial drugs and hematin, preventing its incorporation into β-hematin.[8,9]

An increased concentration of a complex yields a reduced Soret peak of the hemin. The highest reduction (hypochromic effect) for complex **1** was 45% (Table 4). Based on the log *K*

Table 4. Experimental design, log *K* values derived from hemin titration and IC_{50} values derived from β-hematin inhibitory activity (BHIA).

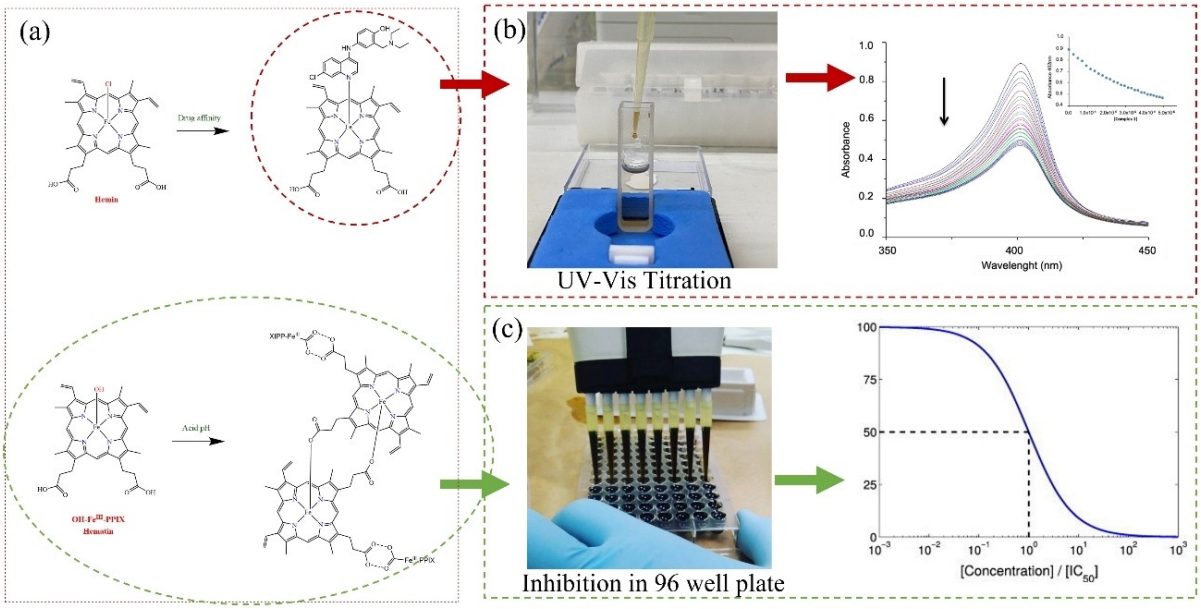

Compounds	Binding to [Cl-Fe^{III}-PPIX]		BHIA, IC_{50} (mean ± S.D. [μM])[c]	
	log *K* (mean ± S.D.)[a]	Hypochromism [%][b]	O-BHIA[d]	R-BHIA[e]
1	5.56 ± 0.23	45	135.6 ± 70.5	190 ± 136
2	5.43 ± 0.04	38	153.4 ± 108.2	208 ± 18
3	5.50 ± 0.12	45	246 ± 66.2	69.7 ± 15
4	5.56 ± 0.03	40	110.5 ± 40.9	62.7 ± 32
amodiaquine	5.69 ± 0.08	45	110.3 ± 57.1	97.6 ± 27
chloroquine	5.80 ± 0.06	53	179.7 ± 17	111.0 ± 17
artemisinin	n.d.	n.d.	> 1000	64.2 ± 9.0

[a] Association constant (log *K*) of hemin [Fe^{III}-PPIX] for the compounds. Determined as the decrease of Soret band of [Fe^{III}-PPIX] in the presence of highest drug ratio in comparison to the absence of compound. [b] Determined as the decrease of Soret band of [Fe(III)-PPIX] in the presence of highest drug ratio in comparison to the absence of compound. [c] β-hematin inhibitory activity (BHIA) was determined 24 h after incubation. [d] Oxidized BHIA (O-BHIA) using hematin [iron(III)] as starting reagent. [e] Reduced BHIA (R-BHIA) using heme [iron(II)] as starting reagent. All values are mean ± S.D. from two to three independent experiments. AQ, amodiaquine free base. CQ, chloroquine-free base. N.D. = not determined; S.D. = standard deviation.

values, it was observed that the affinity of all the metal complexes **1**–**4** for binding to hemin is strong and similar to that observed for AQ. Of note, none the ruthenium or gold precursors (without AQ in their chemical composition) displayed a measurable affinity for hemin. These results agree with those obtained for metal–CQ complexes, which interact similarly to CQ with hemin and presents potent antimalarial activity.[13–17]

β-hematin inhibitory activity (BHIA) was assayed in ferric hematin (O-BHIA) and ferrous heme (R-BHIA) conditions[38] and IC_{50} values derived from BHIA were determined (Table 4). Metal complexes **1**–**3** displayed inhibitory activity against ferric hematin (O-BHIA) that was half as potent as that of AQ. In contrast, the gold complex **4** was in practice equipotent to AQ in inhibiting β-hematin formation and this equipotency was observed in both assays. Based on these IC_{50} values, we can infer that these metal complexes are inhibitors of β-hematin crystal formation as potent as AQ. This is consistent with their strong binding affinity to soluble hemin (log *K*). Interestingly, the ruthenium-phosphine complex **3** was more potent in inhibiting β-hematin when assayed for ferrous heme than for ferric hematin. We speculate that the glutathione present in the R-BHIA assay may have caused a chemical reduction of phosphine in this case.

Discussion

AQ is a potent antimalarial 4-aminoquinoline agent and an important partner drug in artemisinin combination therapy for malaria treatment.[39] However, side effects like acute hepatotoxicity and agranulocytosis have limited its use. Many organic medicinal chemistry approaches have focused on obtaining new analogues of AQ to solve its toxicity problem.[23–25] In this work, we have taken advantage of AQ as a ligand to design metal complexes not just to improve the antimalarial activity, but also to broaden the spectrum of activity in the *Plasmodium* life cycle. Four metal complexes **1**–**4** containing AQ as a

biologically active ligand were synthesized and submitted to thorough chemical characterization. The pharmacological evaluation of antimalarial activity revealed some dissimilarities among the metal complexes **1–4**, denoting that they could work like an AQ delivery system or like a metal-quinoline conjugate endowed with antimalarial properties unlike AQ.

The chemical characterization of the metal complexes **1–4** showed that AQ coordinated to the transition metals through its quinolinic nitrogen. This deserves mention since the hydroxy group present in AQ could represent a potential site for metal coordination. Not only was AQ coordinated exclusively through its quinolinic nitrogen, but this coordination sphere also remained stable upon incubation for 48 h at 37 °C in DMSO or in a mixture of DMSO and culture medium, where no ligand exchange reactions were inferred by NMR or UV-vis analyses. The strong chemical stability in solution for the ruthenium and gold complexes **1–4** is attributed to the great affinity and chemical stabilization of quinolinic ligands for the metal atom center; this is broadly consistent with the prior literature.[20,21]

The pharmacological evaluation of the antimalarial properties of the complexes **1–4** found that the coordination of AQ to transition metals can conserve the overall antimalarial properties of metal-free AQ. This is achieved without affecting cytotoxicity for mammalian cells and providing a range of selectivity indices comparable to AQ. Of the four complexes, ruthenium(II) complex **3** and the gold(I) complex **4** were found to be the most selective antiplasmodial agents. Formal possibilities to explain the structure–activity relationships for complexes **1–4** might rely on the fact that complex **1**, carrying two chlorido ligands, presented the lowest selectivity index, probably because these chlorido ligands can undergo ligand exchange reactions in the cell environment, as was observed in the conductivity experiments, generating species presumably affecting both parasite and host cell targets. For complex **3**, the most selective ruthenium complex among them, it is possible that this works like a drug delivery system, releasing AQ for the parasites cells. This is based on the fact that this compound displayed cell cytotoxicity and antimalarial activity quite similar to AQ treatment. Meanwhile, the gold(I) complex **4** – the most potent and selective of the four – displayed antimalarial activity in multiple assays (in vitro and in vivo) that was more potent and efficacious than AQ treatment. Interestingly, the potency enhancement of complex **4** versus AQ treatment was achieved in AQ-sensitive parasites, which means it was not due to a reversal of drug resistance, as observed for CQ analog ferroquine.[40] Moreover, a gain in lipophilicity for metal complex **4** versus metal-free AQ would unlikely explain the observed potency enhancement, since complex **4** is not the most lipophilic of the complexes. A plausible explanation is that the gold-quinoline conjugate is endowed with a mechanism of action of antimalarial activity that is not reproduced by AQ treatment. In fact, the literature reports that gold complexes can affect *Plasmodium* redox homeostasis by inhibiting flavoenzymes,[41,42] not investigated here. Future work needs to be done to determine the underlying antiplasmodial activity of gold(I) complex **4** at the phenotypic and molecular levels.

It is broadly accepted that antimalarial 4-aminoquinoline drugs bind to soluble and insoluble hematin species, forming quinoline-hematin conjugates responsible for blocking the crystallization of hemozoin. Multiple studies have shown that quinolinic nitrogen can covalently bind to iron(III) from hematin species.[8,9,43] All the metal complexes **1–4** studied exhibited a strong affinity for binding to hemin in a fashion similar to that observed for AQ. This strong affinity is achieved even though the quinolinic nitrogen of AQ is coordinated to ruthenium/gold in complexes **1–4** and these metal-nitrogen bonds are remarkably stable in DMSO and a mixed aqueous medium in a neutral pH, which is a medium very similar to that employed for determining the association of drugs for soluble hematin species (i.e., hemin chloride). Two potential formal explanations of this observed affinity are that the chemical speciation of the metal complexes is different in the presence of hemin or that the AQ ligand in the metal complexes can interact with hemin through binding sites other than quinolinic nitrogen. Although the exact site where metal complexes **1–4** can bind to hemin is still a matter of further investigation, their observed affinity in interacting with hemin is consistent with the prior literature.[10–20]

Finally, we should place the importance of structural modifications on 4-aminoquinolines such as AQ and CQ in the current context of malaria research. These are still important drugs for therapy and as structural prototypes for drug development. A main limitation of AQ is that it can undergo hepatic metabolism by forming a quinone imine metabolite of presumably toxic effect for patients;[23] in fact, many of the structural modifications to AQ have been made to overcome the formation of this toxic metabolite.[23–25] In addition to this, there is an increasing cross-resistance of CQ by AQ in many endemic areas.[44] Therefore, strategies that can overcome both drug toxicity and drug resistance are appealing. Two of the most compelling pharmacological models for explaining the activity of metal complexes carrying bioactive ligands are the complexes behaving as a drug delivery system, where the ligand is released in ligand exchange reactions,[45,46] and the complexes behaving as a delivery system and upon releasing, the resulting metallic species behaving as a drug itself, in parts because these metallic species can have intrinsic reactivity in binding molecular targets.[47,48] Here, we have shown convincing chemical and pharmacological data for the chemical versatility of AQ as a key ligand for developing metal complexes. These metal complexes can reproduce the antiplasmodial phenotype and the mode of action of AQ, but they can also open new possibilities for revisiting the chemistry and mechanism of AQ for malaria intervention.

Conclusions

We have reported on four new AQ metal complexes, [Ru(Cl)$_2$(AQ)(η^6-*p*-cymene)] (**1**), [Ru(AQ)(η^6-*p*-cymene)(2,2′-bipyridine)](PF$_6$)$_2$ (**2**), [Ru(Cl)(AQ)(η^6-*p*-cymene)(PPh$_3$)]PF$_6$ (**3**) and [Au(AQ)(PPh$_3$)]PF$_6$ (**4**), and fully characterized them by analytical and spectral methods (elemental analysis, UV-vis, FTIR, con-

ductivity, mass spectrometry, and NMR). Our analyses indicate that the AQ ligand binds to the metal center through the nitrogen from the quinoline motif. Importantly, AQ remained stable as a ligand in all the Ru^{II} and Au^{I} complexes, even in the presence of coordinating solvents. For the auxiliary ligands, only in complex **1** was there an exchange reaction of chlorido ligand by polar solvents. The four metal–AQ complexes exhibited a strong affinity for binding to hemin in a similar fashion to AQ. Additionally, the conjugation of ruthenium and gold to AQ produced coordination compounds with well-defined properties as antiparasitic agents with a multiple-stage antimalarial profile, acting on different stages of the *Plasmodium* life cycle. From the in vivo assays, reduced parasitemia was observed in the animals and a subsequent increase in survival after treatment with complexes **3** and **4**. The in vivo efficacy data presented here are of relevance to understanding the applicability of metal complexes for treating parasitic infectious diseases, as the literature on this matter is relatively scarce. Finally, it is important to highlight that although our study made advances in the medicinal inorganic chemistry arena, it has the limitation that multiple-stage activity was modest in terms of potency and only demonstrated in in vitro models. Further studies are therefore needed to demonstrate in vivo efficacy in other stages apart from the asexual blood stages, as are studies aiming to understand the underlying importance of metals in the mechanism of action of AQ.

Experimental Section

Materials and equipment: All the metal complexes were synthesized in an argon atmosphere. The metal salt precursors, amodiaquine dihydrochloride dihydrate, triphenylphosphine (PPh_3), *n*-butanol, ammonium hydroxide, ethylenediaminetetraacetic acid (EDTA), Triton X-100, and solvents were purchased from Sigma-Aldrich. Ammonium hexafluorophosphate (NH_4PF_6) and sodium bicarbonate ($NaHCO_3$) were purchased from Merck. The starting materials $[RuCl_2(\eta^6\text{-}p\text{-cymene})]_2$ and $[RuCl_2(\eta^6\text{-}p\text{-cymene})(PPh_3)]$ were prepared following the method described in the literature.[27,33] The UV-vis spectra were obtained using a Hewlett–Packard 8452 A diode-array spectrophotometer. The microanalyses were performed using a Fisions CHNS EA1108 elemental analyzer. The IR spectra were recorded on a Bomem-Michelson FTIR 102 spectrometer in the 4000–500 cm^{-1} region. Conductivity values were obtained using a Meter Lab CDM2300 instrument in $1x10^{-3}$ mol L^{-1} solutions. 1D and 2D NMR experiments were recorded on a 9.4 T Bruker Avance III spectrometer with a 5 mm internal diameter indirect probe with ATMA™ (Automatic Tuning Matching). AQ free base was employed for in vitro assays and amodiaquine dihydrochloride dihydrate (Sigma-Aldrich) was employed for in vivo assays in mice (dosage of salt was adjusted to free base).

Synthesis of amodiaquine free base (AQFB) and metal complexes 1–4

AQFB: Amodiaquine dihydrochloride dihydrate (2.00 g, 4.30 mmol) was dissolved in water and then $NaHCO_3$ (0.80 g, 9.45 mmol) was added. The precipitation of a greenish solid was immediately observed. The mixture was stirred for 2 h at room temperature, then the solid was filtered off, washed with water, and dried under vacuum.

*$[RuCl_2(AQ)(\eta^6\text{-}p\text{-cymene})]$ (**1**)*: A mixture of $[RuCl_2(\eta^6\text{-}p\text{-cymene})]_2$ (0.244 g, 0.40 mmol) and AQFB (0.41 g, 1.14 mmol) in acetone (25 mL) was stirred for 2 h. The yellow solid obtained was filtered off, washed with cold acetone and diethyl ether, and dried under vacuum.

*$[Ru(AQ)(\eta^6\text{-}p\text{-cymene})(2,2'\text{-bipyridine})](PF_6)_2$ (**2**)*: A mixture of $[RuCl(\eta^6\text{-}p\text{-cymene})(2,2'\text{-bipyridine})]PF_6$ (0.20 g, 0.34 mmol) and NH_4PF_6 (0.12 g, 0.73 mmol) in methanol (50 mL) was stirred for 30 min and then AQFB (0.15 g, 0.42 mmol) was added. The mixture was stirred under reflux for 24 h. An orange-brown solution was obtained and dried under vacuum, then dissolved in dichloromethane to filter off the precipitate formed (NH_4Cl). The final solution was dried under vacuum to obtain an orange-brown solid, which was washed with diethyl ether and hexane twice and dried under vacuum.

*$[RuCl(AQ)(\eta^6\text{-}p\text{-cymene})(PPh_3)]PF_6$ (**3**)*: A solution of $[RuCl_2(\eta^6\text{-}p\text{-cymene})(PPh_3)]$ (0.16 g, 0.27 mmol) in methanol (30 mL) was stirred until completely dissolved. NH_4PF_6 (0.05 g, 0.33 mmol) and ligand AQFB (0.13 g, 0.37 mmol) were added. An orange solution was obtained and dried under vacuum then dissolved in dichloromethane to filter off the precipitate formed (NH_4Cl). The final orange solution was concentrated to c. 2 mL and the solid was precipitated by the addition of hexane. The solid obtained was filtrated off, washed with diethyl ether and hexane, and dried under vacuum.

*$[Au(AQ)(PPh_3)]PF_6$ (**4**)*: In the dark, a solution of $AuClPPh_3$ (0.20 g, 0.40 mmol) in acetonitrile (30 mL) was refluxed under nitrogen until completely dissolved, then $AgPF_6$ (0.10 g, 0.40 mmol) was added. The solution was filtered through celite and collected in an acetonitrile solution containing AQFB (0.18 g, 0,50 mmol). The mixture was stirred and refluxed for 12 h. The solvent was removed completely under vacuum. The final yellow solid was washed in diethyl ether and dried under vacuum.

Characterization of AQFB and metal complexes 1–4: This can be found in the Supporting Information.

Determination of association constant for hemin and β-hematin inhibitory activity: The experimental protocol for the association constant (log *K*) of the metal-AQ complexes with hemin chloride $[Cl\text{-}Fe^{III}PPIX]$[37] and their β-hematin inhibitory activity (BHIA)[38] were determined as described in the literature. More experimental details can be found in the Supporting Information.

Evaluation of antimalarial activity through in vitro and in vivo assays

Cytotoxicity against mammalian cells (CC_{50}): In vitro cytotoxicity was assayed against two mammalian cell lines, J774 (murine macrophages) and HepG2 (human hepatocellular carcinoma). The cell lines were maintained in RPMI-1640 (HepG2) or DMEM (J774) containing 10% fetal bovine serum and supplemented with L-glutamine, vitamins, and amino acids in 75-cm^2 flasks at 37 °C, with the medium changed twice weekly. Cell cultures from 60 to 80% confluence were trypsinized, washed in complete medium, and 4×10^4 cells were plated in 100 μL per well with complete medium in 96-well flat-bottom white plates for 24 h at 37 °C prior to the addition of the compounds. Triplicate aliquots of compound and the reference drugs (stock solution in DMSO) covering six different concentrations at twofold dilutions were added to the wells, and plates were incubated for 72 h at 37 °C. Alamarblue reagent (Life Invitrogen) (30 μL) was added in the plates, which were incubated for 4 h at 37 °C. Absorbance at 570 and 600 nm was measured using a Filtermax F3 multi-mode microplate reader (Molecular Devices) and Softmax software. CC_{50} data were obtained from at least two independent experiments for each cell line and analyzed

using Prism 5.01. The selectivity index was estimated using the CC_{50} values from mammalian cells divided by the IC_{50} obtained against the asexual blood stage of *P. falciparum*.

Antiparasitic activity against asexual blood stages of W2 strain of P. falciparum: Parasites were maintained in culture in RPMI-1640 supplemented with 0.5% AlbuMAX™ II (ThermoFisher, Waltham, MA) and buffered with 25 mM 4-(2-hydroxyethyl)-1-piperazineethanesulfonic acid (HEPES) and 25 mM $NaHCO_3$. Parasites were grown in O-positive human blood (HEMOBA, Brazil) under controlled atmospheric conditions of 10% O_2, 5% CO_2, and 85% N_2 at 37 °C with 95% humidity. 100 μL drug and 100 μL parasitized red blood cells (0.5% final parasitemia and 1.5% hematocrit) was distributed per well into 96-well plates. The plates were incubated for 42 h at 37 °C in the controlled atmosphere. Then, 25 μL tritiated hypoxanthine (PerkinElmer) diluted in RPMI to 0.5 μCi/well was added to each well and incubated for 24 h. Plates were frozen at −20 °C and subsequently thawed and the contents transferred to UniFilter-96 GF/B PEI coated plates (PerkinElmer) using a cell harvester. After drying, 50 μL scintillation cocktail (MaxiLight, Hidex, Turku, Finland) was added to each well, sealed, and the plate was read in a liquid scintillation microplate counter (Chameleon, Turku, Finland). IC_{50} data were obtained from at least two independent experiments for each parasite strain and analyzed using Prism 5.01.

Antiparasitic activity against asexual blood stages of NF54 and K1 strains of P. falciparum: *P. falciparum* CQ-susceptible (NF54) and CQ-resistant (K1) parasites were cultured in RPMI-1640 medium supplemented with 25 mM HEPES, 24 mM sodium bicarbonate (pH 7.3), 0.36 mM hypoxanthine, 100 μg/mL neomycin and 0.5% Albumax II were used to test for compound activity on parasite multiplication using a [^{3}H]-hypoxanthine incorporation assay.[49] Compounds were dissolved in DMSO (10 mM), diluted in hypoxanthine-free culture medium and titrated in duplicates over a 64-fold range (six-step twofold dilutions) in 96 well plates. 100 μL asexual parasite culture (prepared in hypoxanthine-free medium) were added to each well and mixed with the compound to obtain a final haematocrit of 1.25% and a final parasitemia of 0.3%. After incubation for 48 h, 0.25 μCi of [^{3}H]-hypoxanthine was added per well and plates were incubated for an additional 24 h. Parasites were then harvested onto glass-fiber filters using a Microbeta FilterMate cell harvester (Perkin Elmer) and radioactivity was counted using a MicroBeta2 liquid scintillation counter (Perkin Elmer). The results were recorded and expressed as a percentage of the untreated controls. Fifty percent inhibitory concentrations (IC_{50}) were estimated by linear interpolation.[50]

Activity against 3D7 P. falciparum *gametocytes*: Gametocytes were obtained from cultures of asexual parasites by increasing parasitemia without adding fresh red blood cells.[51] The complexes were serially diluted in a 96-well flat bottom plate (concentration range 29.0-0.22 μM) at 100 μL per well. Then, 100 μL 3D7elo1-pfs16-CBG99 gametocytes at 0.5-1% parasitemia and 2% hematocrit were dispensed. Each complex was tested in triplicate, in seven different concentrations. The employed DMSO concentration was not toxic for the gametocytes. Methylene blue was used as a positive control. Plates were incubated for 72 h at 37 °C in a controlled atmosphere (3% O_2, 5% CO_2, 91% N_2); 100 μL culture medium was removed from each well to increase hematocrit; 70 μL resuspended culture was transferred to a black 96-well plate; and 70 μL D-luciferin (1 mM in citrate buffer 0.1 M, pH 5.5) was added (to a final concentration of 0.5 mM of D-luciferin). Luminescence measurements were performed after 10 min with 500 ms integration time (luminometer, model Synergy 4, Biotek). Luciferase activity was taken as a measure of gametocyte viability, and IC_{50} was extrapolated from the nonlinear regression analysis of the concentration–response curve. Percentage gametocyte viability was calculated as 100 × ([OD treated sample−OD blank]/[OD untreated sample−μc-blank]) where "blank" was the sample treated with 500 nM methylene blue, which completely kills gametocytes.

Drug-induced hemolysis: Fresh and uninfected human O^+ erythrocytes (uRBC) were washed three times with sterile phosphate-buffered saline (PBS), adjusted for 1.5% hematocrit, and 100 μL was dispensed in a 96-well round-bottom plate. Then, 100 μL complex previously diluted in DMSO and suspended in PBS were dispensed in the respective wells. Each complex was assayed in triplicate at 50 μM. Untreated cells received 100 μL PBS containing 0.5% DMSO (negative control), while positive controls received saponin (Sigma-Aldrich) at 1% *v/v*. Plates were incubated for 1 h at 37 °C under 5% CO_2. Plates were centrifuged at 1500 rpm for 10 min and 100 μL supernatant was transferred to another plate, in which absorbance was measured at 540 nm using a SpectraMax 190 (Molecular Devices, San Jose, USA). Percentage hemolysis was calculated in comparison to positive and negative controls and plotted against drug concentration generated using GraphPad Prism 5.01. One single experiment was performed.

In vivo blood schizontocidal activity: Male Swiss mice (4-6 weeks) were infected by intraperitoneal injection of 10^6 *P. berghei*-infected erythrocytes (strain NK65/GFP) and randomly divided into groups of five. Each drug was solubilized in DMSO/saline (20:80 *v/v*) prior to administration. Treatment was initiated within 24 h post-infection and given daily for four consecutive days by intraperitoneal injection of 100 μL. Amodiaquine $HCl.H_2O$-treated mice were used as a positive control group, while untreated infected mice were used as a negative control group. The following parameters were evaluated: parasitemia at 4, 5, 6, 7, and 8 days post-infection, and 30-day post-infection (DPI) survival. To ensure a humane end-point, mice displaying symptoms of severe anemia were euthanized prior the 30 DPI follow up. Percentage reduction of parasitemia was calculated as: [(mean vehicle group)−(mean treated group)/(mean vehicle group)] ×100%). Each experiment was performed using no more than four groups. Experiments were conducted in 2018 in accordance with the recommendations of the Ethical Issues Guidelines and were approved (reference number 016/2017) by the local animal ethics committee at Fiocruz Bahia (IGM, Salvador, Brazil).

Ruthenium quantification in blood and plasma by inductively coupled plasma mass spectrometry (ICP-MS): Isogenic uninfected C57BL/6 mice (male, 20–25 g) were randomly divided into groups of four and treated with a single dose of the ruthenium compound **3** (100 mg/kg; 102 μmol/kg) by intraperitoneal injection of 200 μL. At 3 h and 24 h after treatment, the mice received anesthesia (tribromoethanol, 200 mg/kg, intraperitoneal), a 200 μL volume of blood was gently aspirated from the brachial plexus using a heparin-coated tip and transferred into heparinized vials on ice. The blood samples were centrifuged at 2500 rpm at 4 °C for 15 min., and a 100 μL volume of plasma was transferred into 1.5 mL microcentrifuge tubes and maintained at −80 °C until analysis. 200 μL red blood cells was transferred into another microcentrifuge tube and washed three times with PBS. The supernatant was discarded and 200 μL cell pellets were stored at −80 °C until analysis.

Experiments were conducted in 2018 in accordance with the recommendations of the Ethical Issues Guidelines and were approved by local animal ethics committee at Fiocruz Bahia (IGM, Salvador, Brazil; reference no. 016/2017).

Sample digestion and metal quantification. Sample digestion was based on a mixture of 2.0 mL of 0.12 mol L^{-1} HCl solution and an alkaline solution prepared by mixing 4% *v/v* *n*-butanol, 1% *m/v* ammonium hydroxide, 0.1% *m/v* ethylenediaminetetraacetic acid, and 0.05% *v/v* Triton X-100. Ultrapure water (resistivity ≥

18.2 MΩ cm at 25 °C) obtained from a Milli-Q Element water purification system (Merck Millipore) was used throughout. All determinations of metal content were conducted by monitoring the ^{102}Ru or ^{104}Ru signals on an Agilent 7800 ICP-MS equipped with a concentric nebulizer and a Scott double pass spray chamber. A single element Ru standard solution used for ICP-MS calibrations was prepared by diluting 1000 mg L^{-1} Ru (Qhemis, São Paulo, Brazil) in 0.14 mol L^{-1} HNO_3 medium, as well as Rh and Ir used as internal standards. The analytical solutions for calibration contained 0.010-200 μg L^{-1} of each analyte and the internal standards were added at 10.0 μg L^{-1} to analytical calibration solutions, analytical blanks, and samples.

Supporting Information

Chemical characterization data, spectra of complexes **1**–**4**, methods, and raw pharmacological data are available in the Supporting Information.

Author Contributions

study design, L.C.V. and D.R.M.M.; experimental work, L.C.V, M.C.B.S., C.S.P., A.I.B., S.D., M.R.; writing of first draft, L.C.V., M.C.B.S., and D.R.M.M.; review and editing, L.C.V., A.A.B., J.A.N., D.R.M.M., M.R., N.B.; funding acquisition, L.C.V., A.A.B., J.A.N., D.R.M.M., M.N., M.R., N.B. All authors read and approved the final manuscript.

Acknowledgements

We are grateful to the following Brazilian agencies for their financial support: Rio Grande do Sul Research Foundation (FAPERGS, grant 54829.632.62060.05032021), São Paulo Research Foundation (FAPESP, grants 16/23130-5, 21/02522-0, and 17/15850-0), the National Council of Technological and Scientific Development (CNPq Brazil, grant 305388/2022-3), and Proep-Fiocruz Program (Brazil, grant 002-FIO-20-2-25). L.C.V. wishes to thank FAPESP for a postdoctoral fellowship (grant 16/23130-5); M.C.B.S. thanks the Fiocruz CAPES-Print Program for a doctoral scholarship (finance code 001). S.D.-A. and N.B. received funding from Fondazione Cariplo (grant 698 2017–0846, Italy), Ministero dell'Istruzione, dell'Università e della Ricerca (grant PRIN 699 2015.4JRJPP_004, Italy), and Ministero degli Affari Esteri e della Cooperazione Internazionale 700 (Progetti di grande rilevanza, grant 00949-2018, Italy). Christin Gumpp at Swiss TPH for performing in vitro antimalarial efficacy studies is greatly appreciated.

Conflict of Interests

There are no conflicts to declare.

Data Availability Statement

The data that support the findings of this study are available in the supplementary material of this article.

Keywords: amodiaquine · infectious disease · malaria · organometallics · quinoline

[1] R. Bianucci, A. Araujo, C. M. Pusch, A. G. Nerlich, *Acta Trop.* **2015**, ***152***, 176–180.
[2] A. L. Mbouaka, M. Gamble, C. Wurst, H. Y. Jäger, F. Maixner, A. Zink, H. Noedl, M. Binder, *Archaeol. Anthropol. Sci.* **2021**, *13*, 115.
[3] *WHO Malaria Report 2022*, http://www.who.int/teams/global-malaria-programme/reports/world-malaria-report-2022 (accessed in February 2023).
[4] M. R. Inklaar, C. Barillas-Mury, M. M. Jore, *Trends Parasitol.* **2022**, *38*, 962–974.
[5] S. W. Lindsay, M. T. Thomas, I. Kleinschmidt, *Lancet Global Health* **2021**, *9*, e1325-e1331.
[6] H. Nunes-Cabaço, D. Moita, M. Prudêncio, *Front. Immunol.* **2022**, *13*, 977472.
[7] R. H. Van Huijsduijnen, T. N. C. Wells, *Curr. Opin. Pharmacol.* **2018**, *42*, 1–6.
[8] K. N. Olafsona, T. Q. Nguyena, J. D. Rimer, P. G. Vekilov, *Proc. Natl. Acad. Sci. USA* **2017**, *114*, 7531–7536.
[9] S. Kapishnikova, T. Staalsø, Y. Yangd, J. Leed, A. J. Pérez-Bernáe, E. Pereiroe, Y. Yang, S. Wernerg, P. Guttmanng, L. Leiserowitzh, J. Als-Nielsen, *Proc. Natl. Acad. Sci. USA* **2019**, *116*, 22946–22952.
[10] C. Biot, G. Glorian, L. A. Maciejewski, J. S. Brocard, *J. Med. Chem.* **1997**, *40*, 3715–3718.
[11] C. Biot, L. Delhaes, L. A. Maciejewski, M. Mortuaire, D. Camus, D. Dive, J. S. Brocard, *Eur. J. Med. Chem.* **2000**, *35*, 707–714.
[12] L. Delhaes, C. Biot, L. Berry, L. A. Maciejewski, D. Camus, J. S. Brocard, D. Dive, *Bioorg. Med. Chem.* **2000**, *8*, 2739–2745.
[13] R. A. Sánchez-Delgado, M. Navarro, H. Pérez, J. A. Urbina, *J. Med. Chem.* **1996**, *39*, 1095–1099.
[14] M. Navarro, H. Pérez, R. A. Sánchez-Delgado, *J. Med. Chem.* **1997**, *40*, 1937–1939.
[15] M. Navarro, W. Castro, A. Martínez, R. A. Sánchez-Delgado, *J. Inorg. Biochem.* **2011**, *105*, 276–282.
[16] M. Navarro, W. Castro, M. Madamet, R. Amalvict, N. Benoit, B. Pradines, *Malar. J.* **2014**, *13*, 471.
[17] C. S. K. Rajapakse, A. Martínez, B. Naoulou, A. A. Jarzecki, L. Suárez, C. Deregnaucourt, V. Sinou, J. Schrével, E. Musi, G. Ambrosini, G. K. Schwartz, R. Sánchez-Delgado, *Inorg. Chem.* **2009**, *48*, 1122–1131.
[18] D. R. Melis, C. B. Barnett, L. Wiesner, E. Nordlander, G. S. Smith, *Dalton Trans.* **2020**, *49*, 11543–11555.
[19] S. N. Sovari, T. M. Golding, M. Mbaba, R. Mohunlal, T. J. Egan, G. S. Smith, F. Zobi, *J. Inorg. Biochem.* **2022**, *234*, 111905.
[20] T. S. Macedo, L. Colina-Vegas, M. Da Paixão, M. Navarro, B. C. Barreto, P. C. M. Oliveira, S. G. Macambira, M. Machado, M. Prudêncio, S. D'Alessandro, N. Basilico, D. R. M. Moreira, A. A. Batista, M. B. P. Soares, *Parasitol.* **2016**, *143*, 1543–1556.
[21] T. S. Macedo, W. Villarreal, C. C. Couto, D. R. M. Moreira, M. Navarro, M. Machado, M. Prudêncio, A. A. Batista, M. B. P. Soares, *Metallomics* **2017**, *9*, 1548–1561.
[22] M. Delves, D. Plouffe, C. Scheurer, S. Meister, S. Wittlin, E. A. Winzeler, R. E. Sinden, D. Leroy, *PLoS Med.* **2012**, *9*, e1001169.
[23] P. M. O'Neill, A. E. Shone, D. Stanford, G. Nixon, E. Asadollahy, B. K. Park, J. L. Maggs, P. Roberts, P. A. Stocks, G. Biagini, P. G. Bray, J. Davies, N. Berry, C. Hall, K. Rimmer, P. A. Winstanley, S. Hindley, R. B. Bambal, C. B. Davis, M. Bates, S. L. Gresham, R. A. Brigandi, F. M. Gomez-de-las-Heras, D. V. Gargallo, S. Parapini, L. Vivas, H. Lander, D. Taramelli, S. A. Ward, *J. Med. Chem.* **2009**, *52*, 1828–1844.
[24] E. Paunescu, S. Susplugas, E. Boll, R. A. Varga, E. Mouray, P. Grellier, P. Melnyk, *Med. Chem.* **2008**, *4*, 407–425.
[25] D. S. Ongarora, N. Strydom, K. Wicht, M. Njoroge, L. Wiesner, T. J. Egan, S. Wittlin, U. Jurva, C. M. Masimirembwa, K. Chibale, *Bioorg. Med. Chem.* **2015**, *23*, 5419–5432.
[26] S. Betanzos-Lara, O. Novakova, R. J. Deeth, R. A. M. Pizarro, A. G. J. Clarkson, B. Liskova, V. Brabec, P. J. Sadler, A. Habtemariam, *J. Biol. Inorg. Chem.* **2012**, *17*, 1033–1051.

[27] L. Colina-Vegas, W. Villarreal, M. Navarro, C. R. de Oliveira, A. E. Graminha, P. S. Maia, V. M. Deflon, V. A. G. Ferreira, M. R. Cominetti, A. A. Batista, *J. Inorg. Biochem.* **2015**, *53*, 150–161.
[28] W. J. Geary, *Coord. Chem. Rev.* **1971**, *7*, 81–122.
[29] A. E. Graminha, C. Popolin, J. Honorato de Araujo-Neto, R. S. Correa, K. M. de Oliveira, L. R. Godoy, L. Colina Vegas, J. Ellena, A. A. Batista, M. R. Cominetti, *Eur. J. Med. Chem.* **2022**, *243*, 114772.
[30] K. Nakamoto, *Infrared and Raman Spectra of Inorganic and Coordination Compounds: Part B: Applications in Coordination, Organometallic, and Bioinorganic Chemistry*, 6th ed., Wiley, Hoboken, **2008**.
[31] L. Colina-Vegas, P. L. J. Godinho, T. Coutinho, R. S. Correa, W. de Souza, J. C. R. Fernandes, A. A. Batista, M. Navarro, *New J. Chem.* **2019**, *43*, 1431–1439.
[32] E. Constable, *Chem. Soc. Rev.* **2013**, *42*, 1637–1651.
[33] J. H. de Araujo-Neto, A. P. M. Guedes, C. M. Leite, C. A. F. Moraes, A. L. Santos, R. D. S. Brito, T. L. Rocha, F. Mello-Andrade, J. Ellena, *Batista AA. Inorg. Chem.* **2023**, *62*, 6955–6969.
[34] G. Siciliano, T. R. Santha Kumar, R. Bona, G. Camarda, M. M. Calabretta, L. Cevenini, E. Davioud-Charvet, K. Becker, A. Cara, D. A. Fidock, P. Alano, *Mol. Microbiol.* **2017**, *104*, 306–318.
[35] M. I. Murillo, C. Gaiddon, R. Le Lagadec, *Front. Chem.* **2022**, *10*, 967337.
[36] S. Theiner, A. Schoeberl, A. Schweikert, B. K. Keppler, G. Koellensperger, *Curr. Opin. Chem. Biol.* **2021**, *61*, 123–134.
[37] T. J. Egan, W. W. Mavuso, D. C. Ross, H. M. Marques, *J. Inorg. Biochem.* **1997**, *68*, 137–145.
[38] K. A. Ribbiso, L. E. Heller, A. Taye, E. Julian, A. V. Willems, P. D. Roepe, *Antimicrob. Agents Chemother.* **2021**, *65*, e02137–20.
[39] T. J. Peto, R. Tripura, J. J. Callery, D. Lek, H. D. Trung Nghia, C. Nguon, N. Huyen Thuong, R. W. van der Pluijm, N. T. Phuong Dung, M. Sokha, V. V. Luong, L. T. Long, Y. Sovann, J. Duanguppama, N. Waithira, R. M. Hoglund, P. Chotsiri, N. Hoang Chau, A. Ruecker, C. Amaratunga, M. Dhorda, O. Miotto, R. J. Maude, H. Rekol, K. Chotivanich, J. Tarning, L. von Seidlein, M. Imwong, M. Mukaka, N. P. J. Day, T. T. Hien, N. J. White, A. M. Dondorp, *Lancet Infect. Dis.* **2022**, *22*, 867–878.
[40] F. Dubar, C. Slomianny, J. Khalife, D. Dive, H. Kalamou, Y. Gurardel, P. Grellier, C. Biot, *Angew. Chem. Int. Ed.* **2013**, *52*, 7690–7693.
[41] C. S. Pereira, H. C. Quadros, D. R. M. Moreira, W. Castro, R. I. S. D. Da Silva, M. B. P. Soares, D. Fontinha, M. Prudencio, V. Schmitz, H. F. Dos Santos, M. Gendrot, I. Fonta, J. Mosnier, B. Pradines, M. Navarro, *ChemMedChem* **2021**, *16*, 662–678.
[42] C. S. Pereira, H. C. Quadros, S. Y. Aboagye, D. Fontinha, S. D'Alessandro, M. E. Byrne, M. Gendrot, I. Fonta, J. Mosnier, D. R. M. Moreira, N. Basilico, D. L. Williams, M. Prudêncio, B. Pradines, M. Navarro, *Pharmaceutica* **2022**, *14*, 1251.
[43] E. L. Dodd, D. Tazoo, D. S. Bohle, *Inorg. Chem.* **2017**, *56*, 7803–7810.
[44] F. Nardella, M. Mairet-Khedim, C. Roesch, S. P. Maher, S. Ke, R. Leang, D. Leroy, B. Witkowski, *J. Antimicrob. Chemother.* **2021**, *76*, 2565–2568.
[45] Y. Lu, X. Ma, X. Chang, Z. Liang, L. Lv, M. Shan, Q. Lu, Z. Wen, R. Gust, W. Liu, *Chem. Soc. Rev.* **2022**, *51*, 5518–5556.
[46] A. Levina, D. C. Crans, P. A. Lay, *Pharmaceutica* **2022**, *14*, 790.
[47] K. Kostenkova, G. Scalese, D. Gambino, D. C. Crans, *Curr. Opin. Chem. Biol.* **2022**, *69*, 102155.
[48] I. Amarsy, S. Papot, G. Gasser, *Angew. Chem. Int. Ed.* **2022**, *61*, e202205900.
[49] C. Snyder, J. Chollet, J. Santo-Tomas, C. Scheurer, S. Wittlin, *Exp. Parasitol.* **2007**, *115*, 296–300.
[50] W. Huber, J. C. Koella, *Acta Trop.* **1993**, *55*, 257–261.
[51] L. Cevenini, G. Camarda, E. Michelini, G. Siciliano, M. M. Calabretta, R. Bona, T. R. Kumar, A. Cara, B. R. Branchini, D. A. Fidock, A. Roda, P. Alano, *Anal. Chem.* **2014**, *86*, 8814–8821.

Manuscript received: May 23, 2023
Accepted manuscript online: July 10, 2023
Version of record online: August 18, 2023